Improved pool fire-initiated domino effect assessment in atmospheric tank farms using structural response

Improved pool fire-initiated domino effect assessment in atmospheric tank farms using structural response

Md. Tanjin Amin[1], Giordano Emrys Scarponi[2], Valerio Cozzani[2*], Faisal Khan[1,*]

[1]Mary Kay O'Connor Process Safety Center,
Artie McFerrin Department of Chemical Engineering,
Texas A&M University, College Station, TX 77843-3122, USA.

[2]Laboratory of Industrial Safety and Environmental Sustainability,
Department of Civil, Chemical, Environmental and Materials Engineering,
University of Bologna, via Terracini 28 40131 Bologna, Italy.

*Corresponding author's email: fikhan@tamu.edu, valerio.cozzani@unibo.it

Abstract:

Domino effects are severe accident scenarios affecting storage tanks and are often initiated by pool fires. Flame engulfment and heat radiation are the two major sources triggering domino effect. Threshold-based and probit-based methods are widely used to assess the possibility and probability of a secondary accident. These methods are also a part of advanced methods devoted to examining synergic or coupling effects. The current work examines (i) how effective the threshold-based methods are and (ii) how accurate the current time to failure (TTF) estimation models are, which are the basis of probit-based methods. The results suggest that threshold-based methods are not pertinent for the quantitative assessment of domino effect and that significant improvement can be made in the existing TTF prediction models using site-specific structural response data. A new set of equations for TTF estimation using data analytics is proposed. Application to 4,080 pool fire scenarios demonstrates that the newly developed model can improve the TTF prediction performance compared to the existing models (around 22% in terms of R^2). In addition, a method has been proposed and validated to correlate time with the failure probability for time-dependent domino effect assessment, which is a limitation of probit-based methods. The current work unveils new insights into the empirical models used for domino effect assessment.

Keywords: *Domino effect*, *pool fire*, *time to failure*, *lumped parameter model, optimization*.

1. Introduction

Process industries, which encompass chemical plants, refineries, and other manufacturing facilities, help modern society by providing several essential products and energy sources that propel the world (Rudberg et al., 2013). However, these industries are not exempt from inherent risks, particularly the daunting challenge of the domino effect (Abdolhamidzadeh et al., 2011; Reniers and Cozzani, 2013). The domino effect refers to a chain reaction of escalating incidents within or across process industry units, triggered by an initial event, with the potential to lead to severe accidents and catastrophic consequences (Necci et al., 2015; Xu et al., 2023). It is a high-impact low-probability (HILP) event that has the potential to cause more damage compared to a single accident (Amin et al., 2019; Rad et al., 2014). A good process safety management system should include domino effect mitigation and prevention plans (CCPS, 2000; Li et al., 2017; Swuste et al., 2019).

Though the Texas City disaster (1947) is regarded as the first documented domino accident, regulations on domino effect prevention were introduced starting with the 1982 Seveso regulations in the European Union (Cozzani and Reniers, 2021; Khan et al., 2021a). To respond to the process safety concerns raised in Europe due to this accident, the European Union (EU) introduced the first Seveso Directive (82/501/EEC), which included measures to prevent the reoccurrence of such accidents (Directive, 1982). This directive was further updated in 1996 and 2012 (Directive, 2012, 1997). The Occupational Safety and Health Administration (OSHA) also guided industries on mitigating the consequences of domino effects in 29 CFR 1910.119 (OSHA, 1994). Nevertheless, domino accidents kept occurring around the world. The 2005 Buncefield oil depot explosion in the UK, the 2005 Texas City Refinery Explosion in the USA, the 2009 Caribbean Petroleum Corporation (CAPECO) fire and explosion in Puerto Rico, the 2015 Tianjin explosions in China, the 2019 Intercontinental Terminal Company (ITC) Deer Park fire in the USA, and the 2020 Beirut explosion in Lebanon are some of the notable domino accidents in the past couple of decades.

Fire incidents, including pool and jet fires, play a significant role in the escalation of accidents, accounting for a substantial portion of domino effects (Guo and Wang, 2023). Fires are responsible for nearly 43% of all domino effects, with pool fires being the more prevalent scenario, triggering around 80% of the fire-driven chain of events (Abdolhamidzadeh et al., 2011). Tank farms, common in process industries, are considered more vulnerable to domino effects compared to other types of storage facilities due to the substantial quantities of hazardous chemicals that are commonly stored in these tanks and to the limited safety distances among tanks. In specific circumstances, a fire in a tank can spread to others (Cui et al., 2022).

Heat radiation and fire engulfment are the escalation vectors potentially triggering domino effects in pool fire scenarios. Among these two, heat radiation is the dominant cause of domino accidents in tank farms due to pool fires (Cozzani et al., 2005; Hemmatian et al., 2014; Santana et al., 2021).

The current literature frequently uses threshold-based and probit-based approaches for domino effect assessment (Cozzani and Reniers, 2021; Khan et al., 2021a). In the threshold-based methods, a cut-off value is considered the domino effect's initiating point. No escalation of a secondary accident is expected unless this value is reached. For example, the National Fire Protection Association (NFPA) suggested 30 kW/m^2 as the threshold (Benedetti and May, 1997). The other widely used thresholds are 15 kW/m^2 and 37.50 kW/m^2 (Cozzani et al., 2006; DNV, n.d.; Kadri et al., 2013). A list of threshold values used in different equipment can be found in the review by Alileche et al. (2015). Although threshold-based approaches are simple to use and crucial to support preliminary hazard screening activities, these are not useful in probabilistic domino effect assessment.

Probit models overcome the limitations of threshold-based approaches. Eisenberg et al. (1975) were the first to use probit models for overpressure impact analysis. Cozzani et al. (2001) proposed a probit-based approach, which nowadays has become a standard tool for fire-driven domino effect assessment (Ding et al., 2022, 2020, 2019; Khakzad and Reniers, 2015; Zhang et al., 2019). The time to failure (TTF) is the most important parameter in this model. TTF measures the time that the target equipment can withstand the escalation vector before failure. Once TTF is calculated, the probability of a domino effect is estimated using the probit model. The existing probit-based technique only allows scenario-specific damage probability estimation. Therefore, it is generally not recommended for time-dependent domino effect assessment, that require the use of improved models (Zhou et al., 2021). Also, to develop an accurate probit model through regression analysis, it is required to know what percentage of damage is expected for a certain value of escalation vector, which is mostly done using available data in the public domain. Generally speaking, determining an equipment's damage percentage is arduous.

In addition to the above approaches, computational fluid dynamics (CFD), thermal response, and graph-based methods are also used for domino effect assessment. CFD-based approaches allow modelling of a wide range of complex geometries at the cost of computational burden (Iannaccone et al., 2021; Jujuly et al., 2015; Yang et al., 2020). Thus, they are not appealing from the practitioners' point of view, and their use is currently limited to academic research. The thermal response models mostly use finite element analysis (FEA) to assess the TTF due

to constant or varying heat loads (Landucci et al., 2009; Yang et al., 2023). Bayesian network (BN) and Petri net (PN) are the widely used tools for graph-based analysis. These tools allow modelling of dynamic scenarios considering dynamic evolutions (Kamil et al., 2019; Khakzad, 2015; Zhou and Reniers, 2022).

In recent years, the synergic effect of multiple hazards (e.g., fire and explosion or double pool fire) on the domino effect has drawn researchers' attention (Ding et al., 2019; He and Weng, 2022; Hou et al., 2022; Li et al., 2023, 2021). The general finding of these works is a higher domino effect possibility compared to that of a single source effect. Time-dependent domino effect assessment has also been focused on in recent studies (Jia et al., 2017; Cozzani and Reniers, 2021; Khan et al., 2021b). However, compared to other areas, it has been less studied yet.

Threshold-based and probit-based models are the basis for several recent works mentioned above. For instance, Khan et al. (2021b) developed an analytical model for time-dependent damage probability estimation using the available damage thresholds. Li et al. (2023) used these thresholds as an important building block to their method to assess the domino effect in storage tank farms under the synergistic effect of explosion and fire. Yang et al. (2020) used the equation proposed by Cozzani et al. (2005) to determine the TTF due to heat load from a pool fire. The authors also used the probit model to determine a domino effect's probability. The same probit model by Cozzani et al. (2001) was used for the domino effects analysis of synergistic effect in the work by Li et al. (2021). Ricci et al. (2021) followed a similar approach to calculate safety distances between vegetation and equipment items in wildland-industrial interface areas.

Though threshold-based and probit-based methods are simpler to use and have advanced the field notably, less focus was on the following issues:

i. How efficient are the threshold-based models for domino effect assessment?
ii. Can the existing models for TTF estimation be improved?
iii. Can the TTF be used to predict dynamic domino effect assessment?

The current work has addressed these questions by (i) comparing the failure behaviour against the existing thresholds and (ii) developing new equations for TTF computation and time-dependent domino effect analysis. The results suggest that in quantitative risk assessment studies, the threshold-based approaches should be revised and if possible, avoided. The new TTF models can predict the domino effect better than the existing ones.

The rest of the paper is organized as follows: Section 2 describes the proposed method with step-by-step illustrations. Section 3 validates the developed models using a couple of case

studies. The results and comparative study among the available models are demonstrated in Section 4. Finally, Section 5 summarises key findings and future direction and concludes the paper.

2. The Proposed methodology for domino effect assessment

A methodology has been developed to assess the dynamic failure probability of an atmospheric tank due to heat radiation generated by a pool fire. The methodology comprises four steps and is shown in Figure 1. These four steps are described in sub-sections 2.1-2.4.

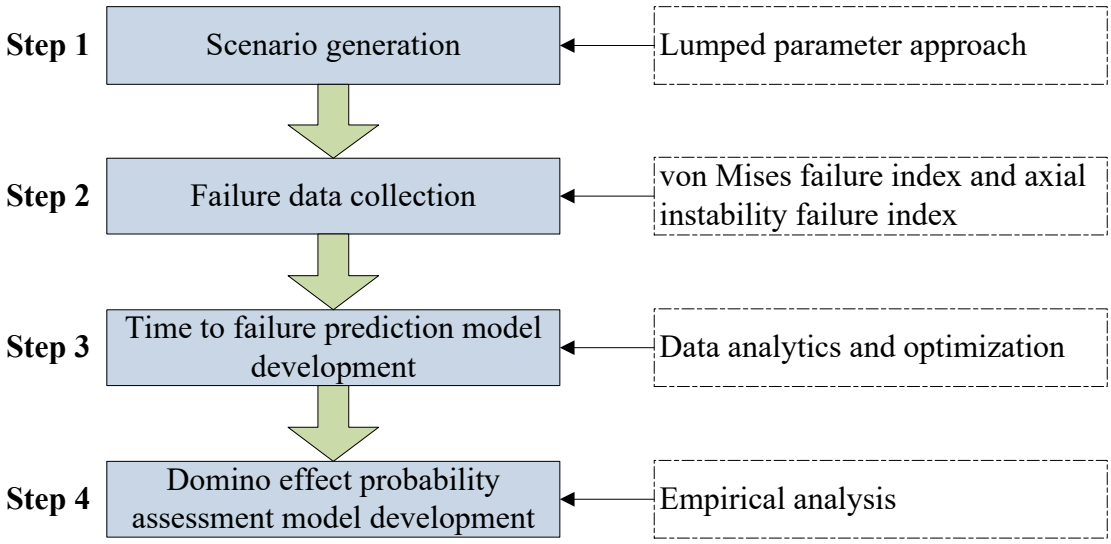

Figure 1: The proposed methodology's overview.

2.1. Scenario generation

The methodology starts with generating atmospheric tank failure scenarios due to pool fire exposure. Time to failure depends both on the features of the tank (design feature and operating conditions, such as filling level) and the heat load received from the fire. In turn, the latter depends on many factors (e.g., pool diameter, distance from the heat source, burning fuel type, wind velocity and direction, percentage of flame covered by the foot, and view factor). The solid flame and CFD models are the most common approaches to estimating heat loads (Yang et al., 2020). While CFD enables modelling complex geometries, it is computationally expensive, even with high-performance computing capacities. In the present work, the heat load from the fire is an input, while the time to failure is calculated based on the tank features and fire heat load using RADMOD, a lumped parameter model presented by Landucci et al. (2009), validated against FEM analysis results. This significantly reduces the computational time required to generate accident scenarios, with a tolerable reduction of output accuracy.

RADMOD is based on a lumped parameter approach that discretizes the domain in two fluid nodes (liquid and vapour) and two solid nodes (wall in contact with the liquid and wall in contact with the vapour). The tank's external diameter, wall thickness for each shell, height of each shell, filling level, initial temperature, initial pressure, and total heat flux are the input to the model. RADMOD calculates node temperatures, tank pressure (accounting for the liquid head), axial stress, and the equivalent von Mises stress in the steel structure. RADMOD can be used to simulate the fire response of conical roof atmospheric tanks. Figure 2 illustrates how the tank domain is partitioned in RADMOD for atmospheric tanks. The model disregards the presence of any fitting, nozzles, and saddles. Benzene is considered a reference substance in this work. More details about the model are presented by Landucci et al. (2009) and Gubinelli (2005).

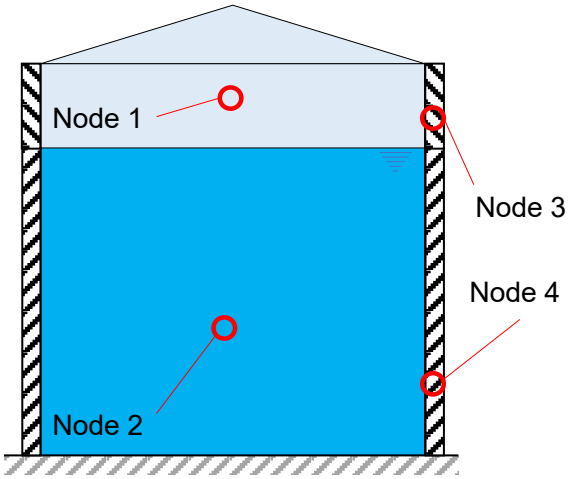

Figure 2: Partition scheme adopted by RADMOD for atmospheric tanks.

The atmospheric tank geometries were set based on the standard provided by the American Petroleum Institute (API) in Table A-2a from *API 650: Welded Steel Tanks for Oil Storage* (API, 1998). A total of 4,080 simulations were carried out considering different combinations of tank diameter and height, shell thickness, filling degree, and total heat flux. The range of model parameters input to RADMOD is displayed in Table 1.

Table 1: Range of input parameters to RADMOD.

Shell diameter, D (m)	Tank height, H (m)	Shell thickness, T (mm)	Filling degree, FD (%)	Total heat flux, I (kW/m^2)
3-66	1.8-18	5-12.50	20-80	9.50-105

Uncertainty is a common phenomenon in domino effect assessment, arising from assumptions and imprecise modelling parameters (Ji et al., 2018; Xu et al., 2023). Conventionally, the heat

load received by the tank is considered constant. However, it may vary with time (Khan et al., 2021b). This work has considered a heat load that may vary within the ±5% limit from the expected heat load. Therefore, each simulation was run thrice considering the ±5% uncertainty in total heat flux received by the target tank. For the same shell diameter, tank height, shell thickness, and filling degree, three heat fluxes: nominal heat flux (I_{nom}), maximum heat flux (I_{max}), and minimum heat flux (I_{min}) are used. I_{nom} is the expected heat flux due to a pool fire. I_{max} and I_{min} are the maximum and minimum heat fluxes, respectively. If I_{nom} is 10 kW/m^2, I_{max} and I_{min} will be 10.50 and 9.50 kW/m^2, respectively.

2.2. Failure data collection

Atmospheric tanks can fail due to plastic deformation and instability. When the equivalent von Mises stress in the tank wall equals the maximum allowable stress, plastic deformation occurs, and the tank fails. In case of instability, the tank fails when axial stress in the tank wall equals a critical stress value. Failures due to plastic deformation and instability can be measured by the von Misses failure index (VMFI) and the axial instability failure index (AIFI). For any node i, the $VMFI_i$ and $AIFI_i$ can be computed using Equations 2 and 3, respectively.

$$VMFI_i = \frac{\sigma_{VM,i}(t) - \sigma_{y,i}(T)}{\sigma_{VM,i}(t=0) - \sigma_{y,i}(T=T_0)} \tag{2}$$

$$AIFI_i = \frac{\sigma_{AX,i}(t) - \sigma_{CR,i}(T)}{\sigma_{MAX,i}(t=0) - \sigma_{CR,i}(T=T_0)} \tag{3}$$

where

$\sigma_{VM,i}(t)$ = von Mises stress at time t for node i

$\sigma_{y,i}(T)$ = yield stress at temperature T for node i

$\sigma_{VM,i}(t=0)$ = von Mises stress at the initial condition for node i

$\sigma_{y,i}(T=0)$ = yield stress at initial temperature for node i

$\sigma_{AX,i}(t)$ = axial stress at time t for node i

$\sigma_{CR,i}(T)$ = critical stress for instability at temperature T for node i

$\sigma_{AX,i}(t=0)$ = axial stress at the initial condition for node i

$\sigma_{CR,i}(T=0)$ = critical stress for instability at initial temperature for node i

Atmospheric tanks are usually made of several shells featuring different thicknesses, the thinner ones at the top and the thicker ones at the bottom, in order to withstand pressure due to the liquid head. RADMOD allows defining of up to three shells. Thus, the check on the above

criteria is done at four different points in the tank wall (as illustrated in Figure 3). Points 1, 2, 3, and 4 are the point connecting the upper shell to the middle one, the middle shell to the lower one, the point at the lower shell's base, and the point at the liquid vapour interface, respectively.

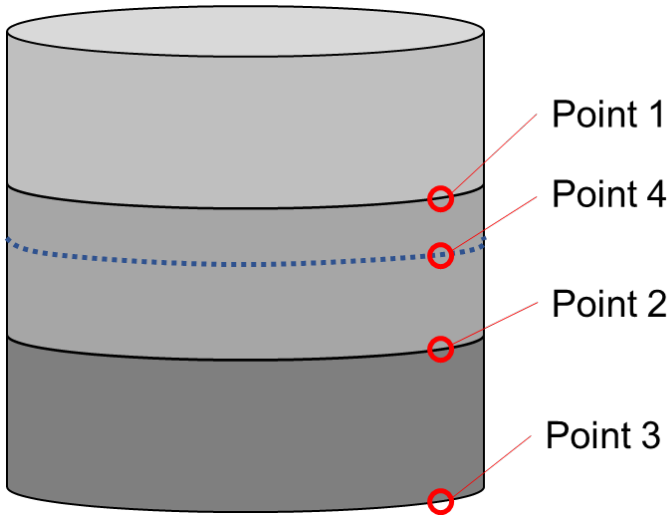

Figure 3: Points where RADMOD performs failure checks for atmospheric tanks.

In order to capture the overall condition of the tank, the minimum $VMFI_i$ and $AIFI_i$ among the four nodes are used.

$VMFI = min_i\ (VMFI_i)$

$AIFI = min_i\ (AIFI_i)$

At initial conditions, $VMFI_i = AIFI_i = 1$

At failure conditions, min $(VMFI_i, AIFI_i) = 0$

The simulation is run till tank failure. In all the cases, the tank failed due to plastic deformation since the Von Mises stress failure criteria were met. The time to failure (TTF) in all scenarios is collected.

2.3. TTF prediction model development

The dataset has five independent variables (shell diameter, tank height, shell thickness, filling degree, and total heat flux) and one dependent variable (time to failure). Shell diameter and tank height can be used to estimate the tank volume, V.

$$V = \frac{\pi}{4} D^2 H \tag{4}$$

Therefore, TTF becomes a function of V, T, FD, and I.

$$TTF = f(V, T, FD, I) \tag{5}$$

Solving Equation 5 falls under a regression analysis problem. It is easier to develop a linear relation. However, it becomes difficult when nonlinearity exists. In this dataset, strong nonlinear relationships are observed among the parameters (see Figure 4). Therefore, nonlinear regression analysis is required.

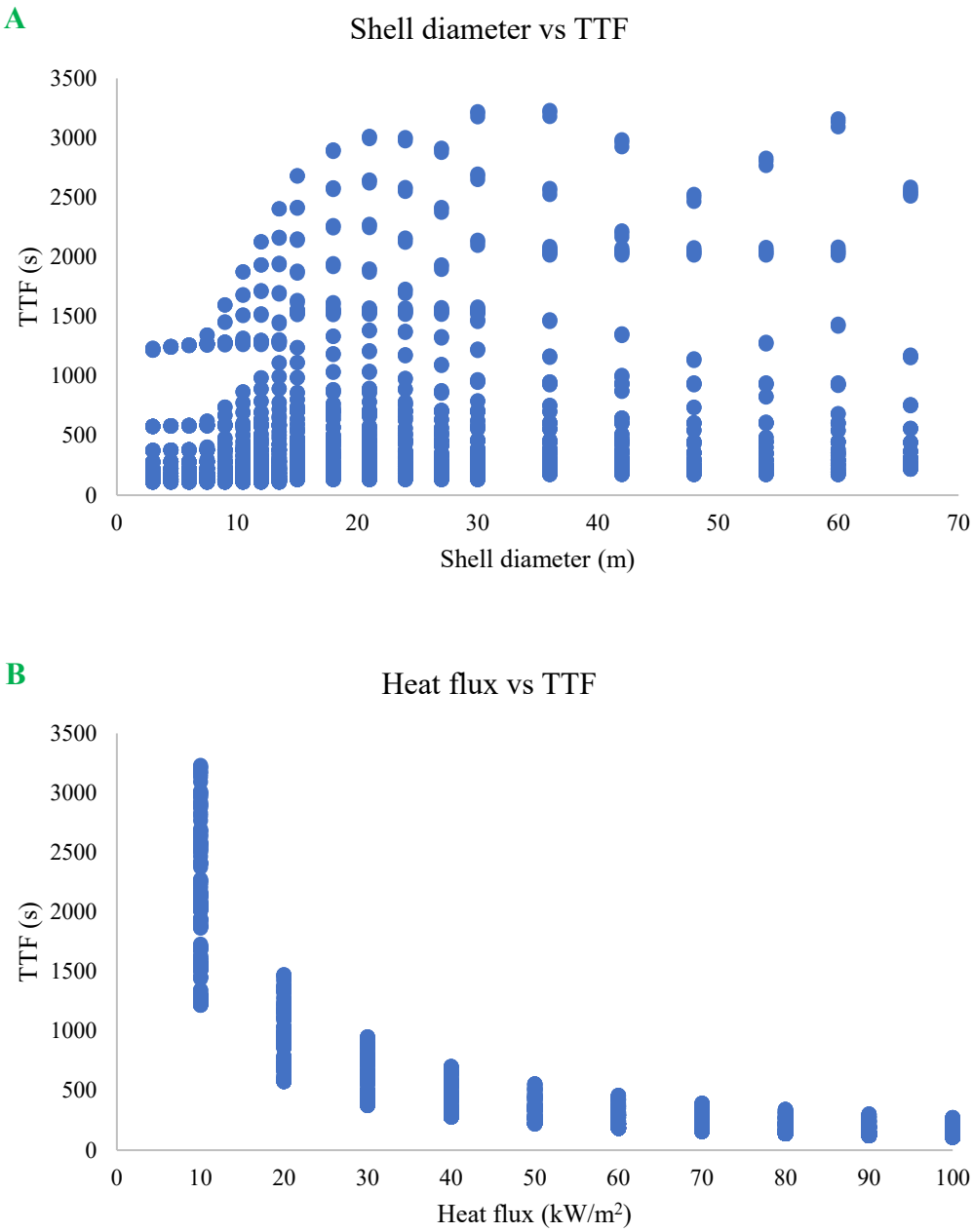

Figure 4: Biplot of (A) shell diameter and time to failure and (B) heat flux and time to failure showing nonlinear relationships.

The following nonlinear correlation can be used to address these issues.

$$TTF = a \times V^b \times T^c \times FD^d \times I^e \tag{6}$$

a, b, c, d, and e are the arbitrary constants.

Taking natural logarithms on both sides of Equation 6,

$$ln(TTF) = \ln(a) + b\,ln(V) + c\,ln(T) + d\,ln(FD) - e\,ln(I) \quad (7)$$

The optimized values for a, b, c, d, and e must be estimated. The normalized difference between the actual and predicted values is minimized to get these model coefficients:

$$\min_{a,b,c,d,e} \sum_{i=1}^{n} \left(\frac{TTF_{predicted} - TTF_{actual}}{TTF_{actual}} \right)^2 \quad (8)$$

where n is the number of scenarios.

A code has been written in Python environment to predict the optimized values for a, b, c, d, and e. The same technique has been adopted to develop the equations for TTF_{min}, TTF_{nom}, and TTF_{max}. The obtained values are reported in Table 2. It should be noted that 3,630 random simulation scenarios were used to develop the TTF prediction models, while the remaining were used to test the model's accuracy. The R^2 values have been used to measure the quality of the fit of the regression models developed using the optimized a, b, c, d, and e values. The results, presented in Table 3, suggest that a good fit is obtained, considering the similar values between the train and test sample and the high R^2 values calculated (>99.90%).

Table 2: Optimized values for a, b, c, d, and e.

	TTF_{min}	**TTF_{nom}**	**TTF_{max}**
a	2489694.657	2656768.598	2829566.646
b	2.84E-03	3.03E-03	3.16E-03
c	9.88E-01	9.88E-01	9.88E-01
d	-1.57E-03	-1.64E-03	-1.71E-03
e	-1.058	-1.062	-1.065

Table 3: R^2 values for train and test scenarios.

	Train scenarios	**Test scenarios**
TTF_{min}	99.94%	99.93%
TTF_{nom}	99.94%	99.92%
TTF_{max}	99.93%	99.91%

Using these optimized a, b, c, d, and e values, the equations for predicting minimum, nominal, and maximum TTF can be developed as presented in Equations 9, 10, and 11, respectively.

$$ln(TTF_{min}) = 14.73 + 2.84 \times 10^{-3}\, ln(V) + 9.88 \times 10^{-1}\, ln(T) - 1.57 \times 10^{-3}\, ln(FD) - 1.058 ln\,(I_{max}) \quad (9)$$

$$ln(TTF_{nom}) = 14.79 + 3.03 \times 10^{-3}\, ln(V) + 9.88 \times 10^{-1}\, ln(T) - 1.64 \times 10^{-3}\, ln(FD) - 1.062 ln\,(I_{nom}) \quad (10)$$

$$ln(TTF_{max}) = 14.86 + 3.16 \times 10^{-3}\, ln(V) + 9.88 \times 10^{-1}\, ln(T) - 1.71 \times 10^{-3}\, ln(FD) - 1.065 ln\,(I_{min}) \quad (11)$$

In Equations 9-11, V, T, FD, and I are in m^3, m, %, and kW/m^2, respectively.

It should be noted that TTF_{max} and TTF_{min} refer to the TTF due to I_{min} and I_{max}, respectively.

2.4. Domino effect assessment model development

The final step is to develop the time-dependent domino effect assessment model. The aim is to develop equations correlating time, t, with the failure probability, P(F). Though yield stress, σ_y can be used to assess the failure probability, it is not a straightforward and quick task to compute σ_y in the field condition. Nonetheless, variables such as the shell diameter, tank height, shell thickness, filling degree, and total heat flux are relatively easier to obtain. Since the TTF is a function of these variables, it can be used to predict the domino effect probability. Hence, most of the current studies adopt TTF in this context (e.g., Cozzani et al. (2005), Landucci et al. (2009), and Zhou et al. (2021)).

The collected dataset suggests that the target tanks fails when time, after initiating the primary accident, falls within the TTF_{min} and TTF_{max}. No failure is noticed until TTF_{min} is reached. The tank can fail at TTF_{nom} if the nominal heat flux is constantly received. However, as mentioned earlier, it may not be realistic to assume that the target tank is constantly receiving a specific heat load, due to inherent variations in pool fire intensity caused by the combustion characteristics of such fires. Nevertheless, all scenarios suggest that failure happens when the tank reaches TTF_{max}. Figure 5 shows the relation between failure probability and time as a function of TTF.

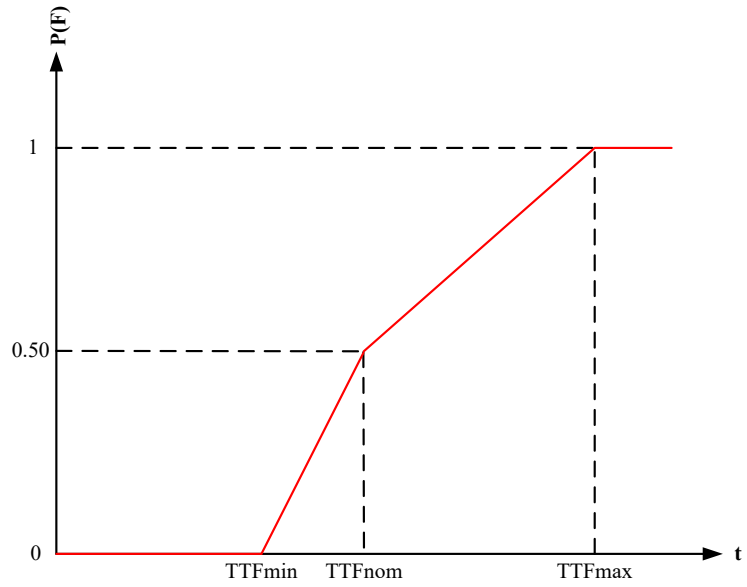

Figure 5: Time vs failure probability plot.

At initial condition, no failure is expected, even with the initiation of the pool fire. The failure probability starts increasing once the atmospheric tank receives the load for a minimum period of time, TTF_{min}. The failure probability keeps increasing towards 0.50 until TTF_{nom} is reached, and it will be unitary at TTF_{max} or any time beyond it. Therefore:

- At any time lower than minimum TTF_{min}, P(F) is 0.
- At any time higher than TTF_{min} and lower than TTF_{nom}, P(F) will increase from 0 towards 0.50.
- At time TTF_{nom}, P(F) is 0.50.
- At any time higher than TTF_{nom} and lower than TTF_{max}, P(F) will increase from 0.50 towards 1.
- At any time equal to or higher than TTF_{max}, P(F) will be 1.

It is worth noting that the probability transition among TTF_{min}, TTF_{nom}, and TTF_{max} can be linear or nonlinear depending on how uniformly the heat loads are received. However, this work has considered linear transitions for the sake of simplicity. Equation 12 can capture the failure phenomena mentioned above and can be used to estimate the failure probability of an atmospheric tank due to a pool fire.

$$P(F)_t = \begin{cases} 0;\ if\ t \leq TTF_{min} \\ 0.50 - s_1 \times (TTF_{nom} - t);\ if\ TTFnom < t < TTF_{min} \\ 0.50;\ if\ t = TTF_{nom} \\ 1 - s_2 \times (TTF_{max} - t);\ if\ TTFmax < t < TTF_{nom} \\ 1;\ if\ t \geq TTF_{max} \end{cases} \quad (12)$$

where $s_1 = \frac{0.50}{TTF_{nom} - TTF_{min}}$ and $s_2 = \frac{0.50}{TTF_{max} - TTF_{nom}}$

3. Model validation: Case Studies

Two case studies have been considered from the test scenarios to test and validate the efficacy of the developed model. The parameters for these scenarios are presented in Table 4.

Table 4: Parameters of validation studies.

Particulates	Case 1	Case 2
Volume, V	12310.06 m^3	12.72 m^3
Shell thickness, T	10 mm	5 mm
Filling degree, FD	50%	50%
Minimum heat flux, I_{min}	95 kW/m^2	9.50 kW/m^2
Nominal heat flux, I_{nom}	100 kW/m^2	10 kW/m^2
Maximum heat flux, I_{max}	105 kW/m^2	10.50 kW/m^2
Minimum time to failure, TTF_{min}	207 s	1163 s
Nominal time to failure, TTF_{nom}	218 s	1229 s
Maximum time to failure, TTF_{max}	230 s	1303 s

Volume, shell thickness, filling degree, and heat flux values are fed into Equations 9-11 to obtain the TTF values. The TTF_{min}, TTF_{nom}, and TTF_{max} values are calculated as 205 s, 216 s, and 227 s, respectively, in the first case study, while TTF values are computed as 1161 s, 1227 s, and 1300 s, respectively, in the second case study. In both cases, the results yield a good match to the actual values. The failure probability is assessed using Equation 12 based on the obtained TTF values. The results are shown in Figures 6(A) and 6(B). It can be seen that the predicted failure probability can closely follow the actual failure probability. The predicted values give a conservative estimate. However, it is better to have an earlier assessment to minimize the consequences. The results imply that the developed model can successfully be used for domino effect assessment due to a pool fire. In particular, since the probability is given as a function of time, the model can be exploited in risk assessment approaches based on the analysis of the dynamic chain of events characterizing the evolution of domino effect scenarios, such as the dynamic Bayesian network approach proposed by Khakzad (2015) and the Petri-nets approach presented by Kamil et al. (2019).

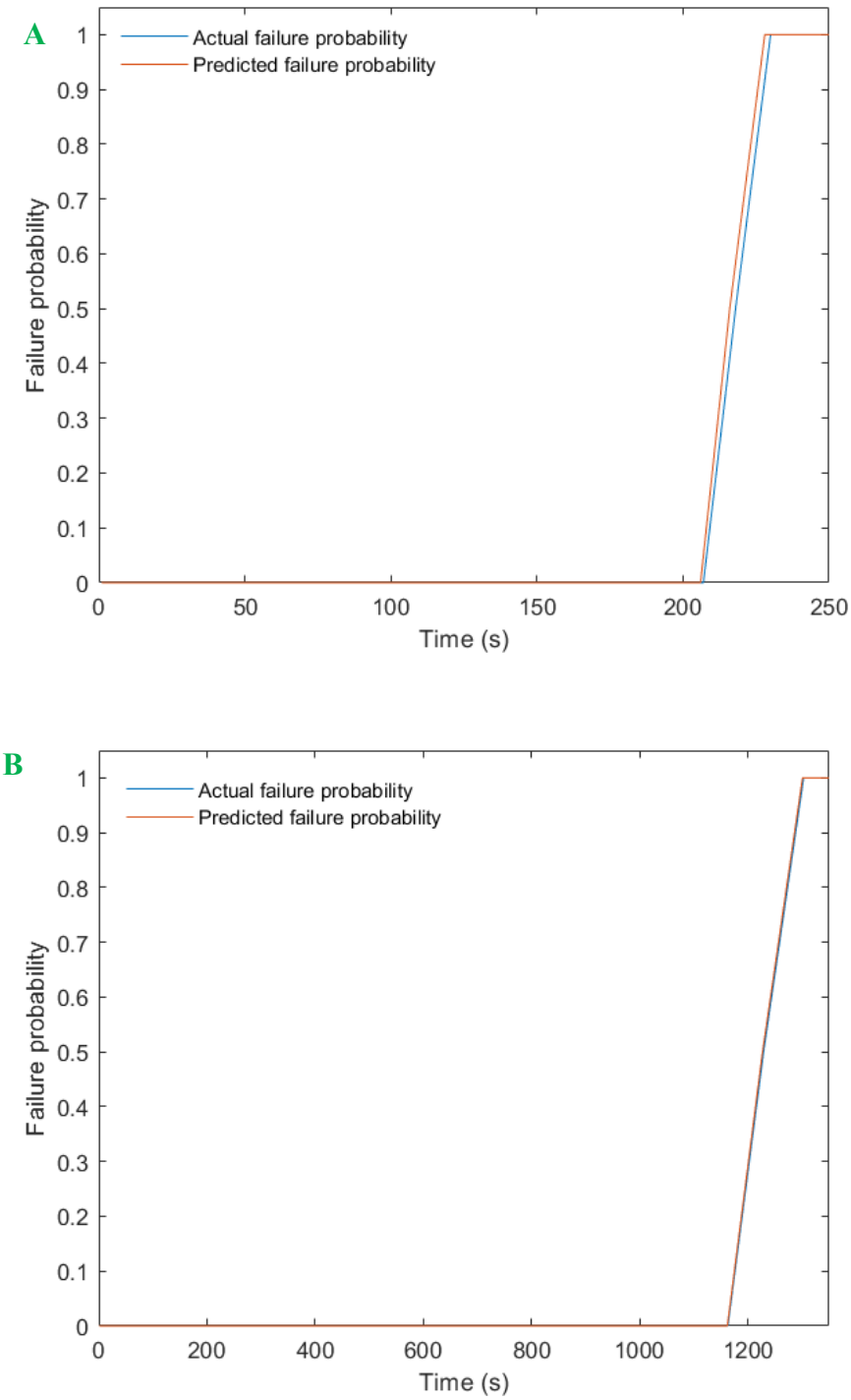

Figure 6: Domino effect probability assessment in (A) case study 1 and (B) case study 2.

4. Results and discussions

The following two important observations have been obtained from the current research.

4.1. Revision of thresholds

Threshold-based methods are widely used in domino effect assessment. For instance, 37.50 kW/m^2 has been suggested as an initiating heat flux for escalating the domino effect in many

sources (DNV, n.d.; Khan and Abbasi, 1998). In the second validation case study, the nominal heat flux received by the tank is 10 kW/m^2, which is lower than this threshold. In fact, 10 kW/m^2 is lower than the majority of the threshold values available in the literature (see Cozzani et al. (2006) and Alileche et al. (2015)).

However, as Figure 7 suggests, the tank can fail even with a heat flux lower than the threshold values if it is constantly subjected to this heat load for a long time period. In this case, the tank did not show any structural change for the first 662 s. Then, it starts losing its plasticity (depicted by lower VMFI). Finally, it fails at 1230 s, as VMFI reaches 0. Thus, threshold-based methods are found misleading in this scenario. Time is confirmed to be an important parameter in domino effect, and it needs to be included while mentioning the thresholds (e.g., 10 kW/m^2 for 20 min), confirming the findings of Cozzani et al. (2006), that proposed time-dependent threshold values for domino effect caused by radiation.

Nevertheless, though some works report time with heat flux as the threshold, most works in the current literature ignore time while mentioning the threshold for domino effect.

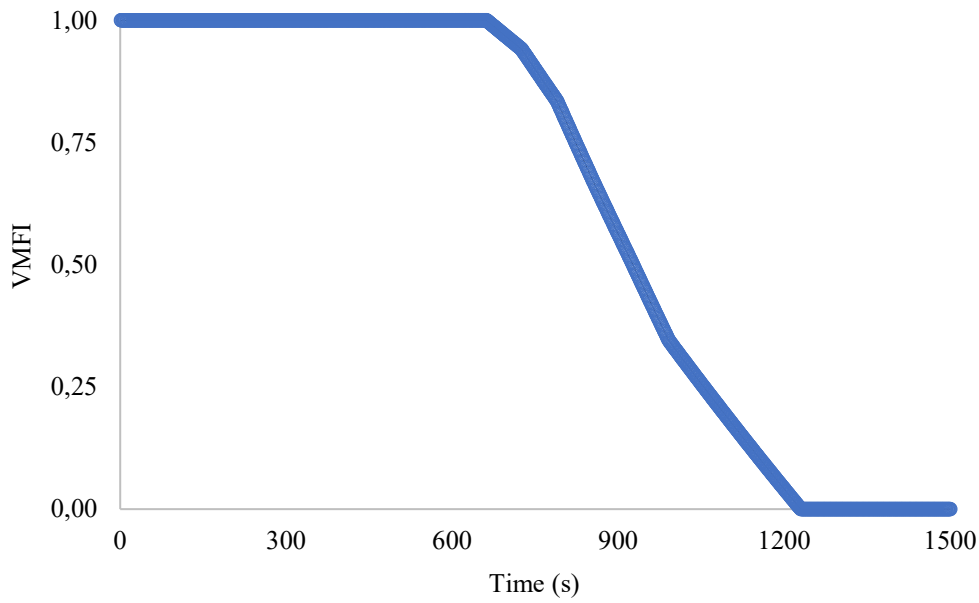

Figure 7: Time vs VMFI in the first case study when the tank is constantly exposed to nominal heat flux.

4.2. Site-specific domino effect model requirement

TTF is the crucial parameter in domino effect modelling. Currently, the simplified model proposed by Cozzani et al. (2005) is the most widely used method (Equation 13) for TTF estimation.

$$ln(TTF) = -1.128(I) - 2.667 \times 10^{-5}V + 9.877 \quad (13)$$

Recently, Yang et al. (2023) have proposed revised TTF models for domino accident analysis under the coupling effect. The authors have proposed a total of three equations. The first analytic model (shown in Equation 14) is developed to estimate the TTF for a tank that receives heat from another tank (where a pool fire has formed) without any coupling effect. This equation from Yang's work has been considered for a fair comparison.

$$ln(TTF) = -1.179(I) - 2.256 \times 10^{-5}V + 9.769 \quad (14)$$

The TTF prediction comparison of this model with the current models to the test scenarios is shown in Figure 8. In addition, Table 5 reports an extensive performance comparison of the overall dataset in terms of commonly used measures for regression analysis, such as R^2, mean absolute error (MAE), and root mean square error (RMSE).

It can be seen that the developed correlation can predict the TTF more accurately. The existing models provide good performance in lower TTF. Nonetheless, their performance notably degrades in case of higher TTF (>1000 s). The R^2, MAE, and RMSE values are significantly improved in the current model. Yang's model provides better performance than Cozzani's model in terms of R^2. However, MAE and RMSE suggest that the latter performs well in case of nominal TTF prediction.

However, the models proposed by Cozzani et al. (2005) and Yang et al. (2023) have been developed considering two variables (volume and heat flux). On the contrary, the current work includes the other crucial parameters (i.e., shell thickness and filling degree). Though, even if it slightly increases the computational complexity, it provides significantly improved results. Using a different range of modelling parameters (e.g., range of tank volume) can be another reason. Typically, a regression model works well within its known boundary. The current models should give good results when the available information falls within the range of values mentioned in Table 1. However, plant-specific information (e.g., fuel type, tank volume, shell thickness, filling degree, heat flux, and time to failure) should be incorporated to get a better prediction.

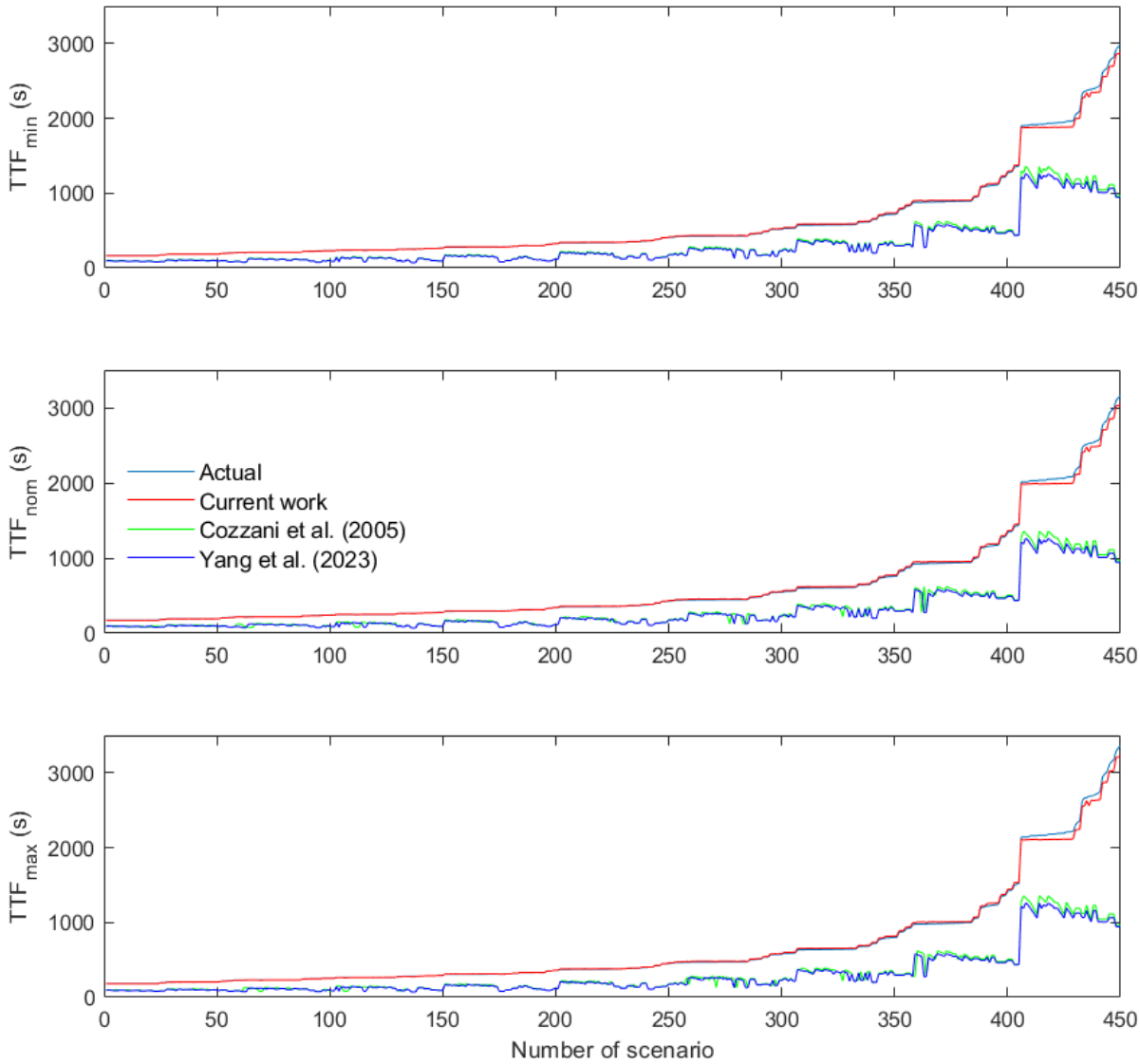

Figure 8: Actual vs predicted TTF by different models for the test scenarios.

Table 5: Performance comparison between the current work and existing TTF prediction models.

Parameter		Current work	Cozzani et al. (2005)	Yang et al. (2023)
R^2	TTF_{min}	99.94%	76.80%	77.84%
	TTF_{nom}	99.93%	76.76%	77.80%
	TTF_{max}	99.92%	76.83%	77.87%
MAE	TTF_{min}	7.73	144.11	135.81
	TTF_{nom}	8.48	122.89	155.27
	TTF_{max}	9.54	132.67	124.55
RMSE	TTF_{min}	16.93	293.19	276.86
	TTF_{nom}	18.59	245.94	309.61
	TTF_{max}	21.03	272.02	257.24

5. Conclusion

This work investigates the accuracy of threshold-based and probit-based methods in assessing cascading events. A total of 4,080 pool fire scenarios in atmospheric tanks have been generated using a lumped parameter modelling approach – a technique that allows simulating scenarios much faster than CFD and has been validated in the work by Landucci et al. (2009). The tank dimensions have been selected according to the guidelines provided by the API. The tanks have been allowed to fail in all scenarios due to heat radiation. The VMFI and AIFI indicators are used as failure indicators, and TTF is used as the measure of structural response. It has been observed that the tanks have failed due to plastic deformation in all cases.

Threshold-based methods are found ineffective for domino effect assessment, as it is observed that a failure may happen with heat radiation lower than the suggested thresholds provided that the exposure to fire lasts for a sufficiently extended time. A new TTF prediction model is developed that can improve probit-based method's prediction accuracy, as it has been observed that the developed model can outperform the existing models by significant margins in terms of commonly used performance indicators, such as R^2, MAE, and RMSE. Also, to overcome probit-based method's limitation in predicting dynamic failure probability, a new method for domino effect assessment in atmospheric tanks due to a pool fire has been proposed. Uncertainty in received heat load has been considered while developing the model. The developed model has been tested and validated in two case studies.

The current model applies to atmospheric tanks and pool fire scenarios. Future works may include extending it to other fire and explosion scenarios and pressurized tanks. Also, the synergic effect of multiple fires or of simultaneous exposure to different types of hazards needs to be considered.

Acknowledgement: The authors thankfully acknowledge the funding support from the Mary Kay O'Connor Process Safety Center (MKOPSC) at Texas A&M University, TX, USA and from University of Bologna, Italy.

References:

Abdolhamidzadeh, B., Abbasi, T., Rashtchian, D., Abbasi, S.A., 2011. Domino effect in process-industry accidents - An inventory of past events and identification of some patterns. J. Loss Prev. Process Ind. 24, 575–593. https://doi.org/10.1016/j.jlp.2010.06.013

Alileche, N., Cozzani, V., Reniers, G., Estel, L., 2015. Thresholds for domino effects and safety distances in the process industry: A review of approaches and regulations. Reliab. Eng.

Syst. Saf. 143, 74–84. https://doi.org/10.1016/j.ress.2015.04.007

Amin, M.T., Khan, F., Amyotte, P., 2019. A bibliometric review of process safety and risk analysis. Process Saf. Environ. Prot. 126, 366–381. https://doi.org/10.1016/j.psep.2019.04.015

API, 1998. API Standard 650: Welded Steel Tanks for Oil Storage. American Petroleum Institute.

Benedetti, R.P., May, P.E., 1997. Flammable and combustible liquids code handbook. National Fire Protection Assciation.

CCPS, 2000. Guidelines for chemical process quantitative risk analysis, New York, NY. American Institute of Chemical Engineers (AIChE), New York.

Cozzani, V., Gubinelli, G., Antonioni, G., Spadoni, G., Zanelli, S., 2005. The assessment of risk caused by domino effect in quantitative area risk analysis. J. Hazard. Mater. 127, 14–30. https://doi.org/10.1016/j.jhazmat.2005.07.003

Cozzani, V., Gubinelli, G., Salzano, E., 2006. Escalation thresholds in the assessment of domino accidental events. J. Hazard. Mater. 129, 1–21. https://doi.org/10.1016/j.jhazmat.2005.08.012

Cozzani, V., Mazzoni, A., Gozzi, F., Zanelli, S., 2001. Assessment of probabilistic models for the estimation of accident propagation hazards, in: Proc. ESREL 2001. pp. 807–814.

Cui, X., Zhang, M., Pan, W., 2022. Dynamic probability analysis on accident chain of atmospheric tank farm based on Bayesian network. Process Saf. Environ. Prot. 158, 146–158. https://doi.org/10.1016/j.psep.2021.10.040

Ding, L., Ji, J., Khan, F., 2020. Combining uncertainty reasoning and deterministic modeling for risk analysis of fire-induced domino effects. Saf. Sci. 129, 104802. https://doi.org/10.1016/j.ssci.2020.104802

Ding, L., Khan, F., Abbassi, R., Ji, J., 2019. FSEM: an approach to model contribution of synergistic effect of fires for domino effects. Reliab. Eng. Syst. Saf. 189, 271–278. https://doi.org/10.1016/j.ress.2019.04.041

Ding, L., Khan, F., Ji, J., 2022. A novel vulnerability model considering synergistic effect of fire and overpressure in chemical processing facilities. Reliab. Eng. Syst. Saf. 217, 108081. https://doi.org/10.1016/j.ress.2021.108081

Directive, C., 2012. Directive, 2012/18/EU on the Control of Major-Accident Hazards Involving Dangerous Substances. Off. J. Eur. Union L 197, 1–37.

Directive, C., 1997. 96/82/EC of 9 December 1996 on the control of major-accident hazards involving dangerous substances. Off. J. Eur. Communities, L 10, 13–33.

Directive, C., 1982. Council Directive 82/501/EEC on the major-accident hazards of certain industrial activities. Off. J. Eur. Communities 1–18.

DNV, n.d. Phast and Safeti for domino assessment [WWW Document]. URL https://www.dnv.com/article/phast-and-safeti-for-domino-assessment-207736 (accessed 6.20.23).

Eisenberg, N.A., Lynch, C.J., Breeding, R.J., 1975. Vulnerability model. a simulation system for assessing damage resulting from marine spills. Enviro control inc rockville md.

Gubinelli, G., 2005. Domino effect in the process industries: quantitative methodologies for the evaluation of consequences, 2005. Ph. D. thesis in Chemical Engineering. University of Pisa, Pisa.

Guo, L., Wang, Z., 2023. Analysis of uncertainty propagation path of fire-induced domino effect based on an approach of layered fuzzy Petri nets. Chem. Eng. Sci. 268, 118410. https://doi.org/10.1016/j.ces.2022.118410

He, Z., Weng, W., 2022. Synergistic effects on the physical effects of explosions in multi-hazard coupling accidents in chemical industries. J. Loss Prev. Process Ind. 77, 104800. https://doi.org/10.1016/j.jlp.2022.104800

Hemmatian, B., Abdolhamidzadeh, B., Darbra, R.M., Casal, J., 2014. The significance of domino effect in chemical accidents. J. Loss Prev. Process Ind. 29, 30–38. https://doi.org/10.1016/j.jlp.2014.01.003

Hou, S., Luan, X., Wang, Z., Cozzani, V., Zhang, B., 2022. A quantitative risk assessment framework for domino accidents caused by double pool fires. J. Loss Prev. Process Ind. 79, 104843. https://doi.org/10.1016/j.jlp.2022.104843

Iannaccone, T., Scarponi, G.E., Landucci, G., Cozzani, V., 2021. Numerical simulation of LNG tanks exposed to fire. Process Saf. Environ. Prot. 149, 735–749. https://doi.org/10.1016/j.psep.2021.03.027

Ji, J., Tong, Q., Khan, F., Dadashzadeh, M., Abbassi, R., 2018. Risk-Based Domino Effect Analysis for Fire and Explosion Accidents Considering Uncertainty in Processing Facilities. Ind. Eng. Chem. Res. 57, 3990–4006. https://doi.org/10.1021/acs.iecr.8b00103

Jia, M., Chen, G., Reniers, G., 2017. An innovative framework for determining the damage probability of equipment exposed to fire. Fire Saf. J. 92, 177–187. https://doi.org/10.1016/j.firesaf.2017.05.015

Jujuly, M.M., Rahman, A., Ahmed, S., Khan, F., 2015. LNG pool fire simulation for domino effect analysis. Reliab. Eng. Syst. Saf. 143, 19–29. https://doi.org/10.1016/j.ress.2015.02.010

Kadri, F., Châtelet, E., Chen, G., 2013. Method for quantitative assessment of the domino effect in industrial sites. Process Saf. Environ. Prot. 91, 452–462. https://doi.org/10.1016/j.psep.2012.10.010

Kamil, M.Z., Taleb-Berrouane, M., Khan, F., Ahmed, S., 2019. Dynamic domino effect risk assessment using Petri-nets. Process Saf. Environ. Prot. 124, 308–316. https://doi.org/10.1016/j.psep.2019.02.019

Khakzad, N., 2015. Application of dynamic Bayesian network to risk analysis of domino effects in chemical infrastructures. Reliab. Eng. Syst. Saf. 138, 263–272. https://doi.org/10.1016/j.ress.2015.02.007

Khakzad, N., Reniers, G., 2015. Risk-based design of process plants with regard to domino effects and land use planning. J. Hazard. Mater. 299, 289–297. https://doi.org/10.1016/j.jhazmat.2015.06.020

Khan, F., Abbasi, S., 1998. Models for domino effect analysis in chemical process industries. Process Saf. Prog. 17, 107–123. https://doi.org/10.1002/prs.680170207

Khan, F., Amin, M.T., Cozzani, V., Reniers, G., 2021a. Domino effect: Its prediction and prevention—An overview. Methods Chem. Process Saf. 5, 1–35. https://doi.org/10.1016/bs.mcps.2021.05.001

Khan, F., Amin, M.T., Cozzani, V., Reniers, G., 2021b. Domino effect assessment in the framework of industry 4.0, in: Methods in Chemical Process Safety. Elsevier, pp. 495–517. https://doi.org/10.1016/bs.mcps.2021.05.015

Landucci, G., Gubinelli, G., Antonioni, G., Cozzani, V., 2009. The assessment of the damage probability of storage tanks in domino events triggered by fire. Accid. Anal. Prev. 41, 1206–1215. https://doi.org/10.1016/j.aap.2008.05.006

Li, J., Reniers, G., Cozzani, V., Khan, F., 2017. A bibliometric analysis of peer-reviewed publications on domino effects in the process industry. J. Loss Prev. Process Ind. 49, 103–110. https://doi.org/10.1016/j.jlp.2016.06.003

Li, X., Chen, G., Amyotte, P., Alauddin, M., Khan, F., 2023. Modeling and analysis of domino effect in petrochemical storage tank farms under the synergistic effect of explosion and fire. Process Saf. Environ. Prot. https://doi.org/10.1016/j.psep.2023.06.054

Li, X., Chen, G., Huang, K., Zeng, T., Zhang, X., Yang, P., Xie, M., 2021. Consequence modeling and domino effects analysis of synergistic effect for pool fires based on computational fluid dynamic. Process Saf. Environ. Prot. 156, 340–360. https://doi.org/10.1016/j.psep.2021.10.021

Necci, A., Cozzani, V., Spadoni, G., Khan, F., 2015. Assessment of domino effect: State of the

art and research Needs. Reliab. Eng. Syst. Saf. 143, 3–18. https://doi.org/10.1016/j.ress.2015.05.017

OSHA, 1994. Process Safety Management of Highly Hazardous Chemicals - Compliance Guidelines and Enforcement Procedures.

Rad, A., Abdolhamidzadeh, B., Abbasi, T., Rashtchian, D., 2014. FREEDOM II: An improved methodology to assess domino effect frequency using simulation techniques. Process Saf. Environ. Prot. 92, 714–722. https://doi.org/10.1016/j.psep.2013.12.002

Reniers, G., Cozzani, V., 2013. Domino effects in the process industries: modelling, prevention and managing. Newnes.

Ricci, F., Scarponi, G.E., Pastor, E., Planas, E., Cozzani, V., 2021. Safety distances for storage tanks to prevent fire damage in Wildland-Industrial Interface. Process Saf. Environ. Prot. 147, 693–702. https://doi.org/10.1016/j.psep.2021.01.002

Rudberg, M., Waldemarsson, M., Lidestam, H., 2013. Strategic perspectives on energy management: A case study in the process industry. Appl. Energy 104, 487–496. https://doi.org/10.1016/j.apenergy.2012.11.027

Santana, J.A.D., Orozco, J.L., Furka, D., Furka, S., Matos, Y.C.B., Lantigua, D.F., Miranda, A.G., González, M.C.B., 2021. A new Fuzzy-Bayesian approach for the determination of failure probability due to thermal radiation in domino effect accidents. Eng. Fail. Anal. 120, 105106. https://doi.org/10.1016/j.engfailanal.2020.105106

Swuste, P., van Nunen, K., Reniers, G., Khakzad, N., 2019. Domino effects in chemical factories and clusters: An historical perspective and discussion. Process Saf. Environ. Prot. 124, 18–30. https://doi.org/10.1016/j.psep.2019.01.015

Xu, Y., Reniers, G., Yang, M., Yuan, S., Chen, C., 2023. Uncertainties and their treatment in the quantitative risk assessment of domino effects: Classification and review. Process Saf. Environ. Prot. https://doi.org/10.1016/j.psep.2023.02.082

Yang, J., Zhang, M., Zuo, Y., Cui, X., Liang, C., 2023. Improved models of failure time for atmospheric tanks under the coupling effect of multiple pool fires. J. Loss Prev. Process Ind. 81, 104957. https://doi.org/10.1016/j.jlp.2022.104957

Yang, R., Khan, F., Neto, E.T., Rusli, R., Ji, J., 2020. Could pool fire alone cause a domino effect? Reliab. Eng. Syst. Saf. 202, 106976. https://doi.org/10.1016/j.ress.2020.106976

Zhang, M., Zheng, F., Chen, F., Pan, W., Mo, S., 2019. Propagation probability of domino effect based on analysis of accident chain in storage tank area. J. Loss Prev. Process Ind. 62, 103962. https://doi.org/10.1016/j.jlp.2019.103962

Zhou, J., Reniers, G., 2022. Petri-net based cooperation modeling and time analysis of

emergency response in the context of domino effect prevention in process industries. Reliab. Eng. Syst. Saf. 223, 108505. https://doi.org/10.1016/j.ress.2022.108505

Zhou, J., Reniers, G., Cozzani, V., 2021. Improved probit models to assess equipment failure caused by domino effect accounting for dynamic and synergistic effects of multiple fires. Process Saf. Environ. Prot. 154, 306–314. https://doi.org/10.1016/j.psep.2021.08.020